



European Union's Seventh Framework Programme

Grant Agreement N°: **603521**

Project Acronym: **PREFACE**

Project full title: **Enhancing prediction of tropical Atlantic climate and its impacts**

Instrument: Collaborative Project

Theme: ENV.2013.6.1-1 – *Climate-related ocean processes and combined impacts of multiple stressors on the marine environment*

Start date of project: 1 November 2013

Duration: 48+6 Months

Deliverable reference number and full title: *D12.3: Report of macrozooplankton distributions*

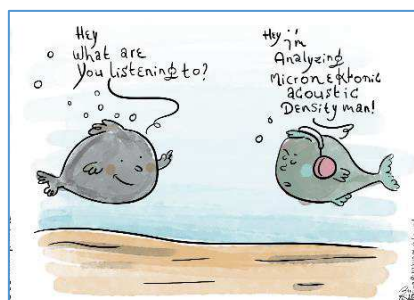
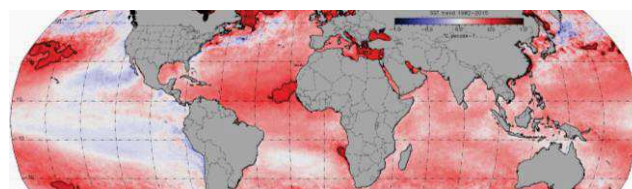
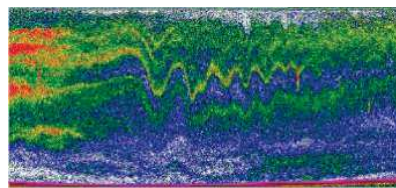
Core theme 5, Work Package 12: *Task 12.3 Comparative analyses of spatiotemporal macrozooplankton distributions along three LMEs of the West coast of Africa related to environmental parameters*

Lead beneficiary for this deliverable: IRD

Due date of deliverable: 30/04/2018

Actual submission date: 27/04/2018

Project co-funded by the European Commission within the Seven Framework Programme (2007-2013)			
Dissemination Level			
PU	Public		
PP	Restricted to other programme participants (including the Commission Services)		
RE	Restricted to a group specified by the Consortium (including the Commission Services)		
CO	Confidential, only for members of the Consortium (including the Commission Services)		X



Contribution to project objectives – with this deliverable, the project has contributed to the achievement of the following objectives (from Annex I / DOW, Section B1.1.):

N.º	Objective	No	Yes
1	Reduce uncertainties in our knowledge of the functioning of Tropical Atlantic (TA) climate, particularly climate-related ocean processes (including stratification) and dynamics, coupled ocean, atmosphere, and land interactions; and internal and externally forced climate variability.	X	
2	Better understand the impact of model systematic error and its reduction on seasonal-to-decadal climate predictions and on climate change projections.	X	
3	Improve the simulation and prediction TA climate on seasonal and longer time scales, and contribute to better quantification of climate change impacts in the region.	X	
4	Improve understanding of the cumulative effects of the multiple stressors of climate variability, greenhouse-gas induced climate change (including warming and deoxygenation), and fisheries on marine ecosystems, functional diversity, and ecosystem services (e.g., fisheries) in the TA.		X
5	Assess the socio-economic vulnerabilities and evaluate the resilience of the welfare of West African fishing communities to climate-driven ecosystem shifts and global markets.	X	

Main Author(s) of this deliverable: Patrice Brehmer (IRD), Hervé Demarcq (IRD), Nolwenn Behagle (IRD), Maik Tiedemann (IRD), Yannick Perrot (IRD), Anne Mouget (IRD), Chloe Migayrou (IRD), Aka Marcel Kouassi (CRO), Uatjavi Uanivi (MFMR), Salahedine El Ayoubi (INRH), Mamadou Ndiaye (IRD), Jens-Otto Krakstad (IMR), Adrien Berne (IRD), and Abdoulaye Sarré (ISRA/CRODT).

Comments on deviations: Data and personnel recruitment issues related to Task 12.3 in the three regions under study (Canary Current Large Marine Ecosystem, Gulf of Guinea LME, and Benguela Current LME) delayed this task and achievement of D12.3 by 6 months. For the CCLME, a PhD student only began in month 37 with the analysis of acoustic EAF Nansen survey data. A postdoctoral scientist was recruited around roughly the same time to focus on acoustic data extraction and analysis in the GCLME, while supporting progress in the other LMEs. The late release of the entire acoustic data base (including missing transect in the ICPC first release) was due to the necessary transformation of the EAF Nansen survey acoustic data into classic raw format from an old aggregated Norwegian binary format. Standard extraction of acoustic data was hindered by the lack of *ad hoc* license or software types for common data extraction and standard processing. However, in PREFACE, IRD provided a Matlab algorithm (methodology recently accepted in “Australian Acoustics”) for data analysis to all ICPC beneficiaries that enabled the planned comparative analysis within PREFACE but will allow for future data analyses at these and other institutions.

Executive Summary: Zooplankton and micronekton are key groups in ocean foodwebs. Both micronekton and macrozooplankton (here further referred to simply as micronekton) are consumers of primary producers, microzooplankton, and detritus, producing dissolved and particulate organic matter, thereby actively contributing to the remineralisation of nutrients. These biological cycles are also key processes in the maintenance of the oxygen minimum zone in upwelling areas (OMZ). Furthermore, micronekton contribute to the export of matter to the ocean sea floor with fast-sinking faecal pellets, via diel vertical migration (DVM). In turn, micronekton are main prey items for a large variety of exploited and non-exploited fishes. Micronekton therefore perform a critical role in structuring higher and lower trophic levels, influencing the population dynamics of exploited species. In past decades, acoustic methods have enabled the extraction of high-resolution information on the biomass and distribution patterns of micronekton.

To study micronekton interannual variability and trend in the three African Atlantic large marine ecosystems (LME), *i.e.*, the Canary Current LME (CCLME), Guinea Current LME (GCLME), and Benguela Current LME (BCLME), particularly over the continental shelf where most fisheries activities occur, we compiled almost 300 000 km of survey transects through 29 surveys carried out by the FRV Fridtjof Nansen. The historical data were converted, cleaned, and echo integrated using *ad hoc* software 'Matecho' developed as open source that enabled collaborative work and applied a standardized method to all surveys.

The environmental data were compiled from remote sensing satellite products. Special analysis was made in the CCLME, making use of a database of vertical probes (water: Temperature, Salinity, and Oxygen). Space-based observations of some major parameters allow a precise synoptic observation of marine ecosystems. Sea surface temperature (SST) has been observed for 36 years and ocean-colour related parameters, such as surface primary productivity, for more than 20 years. The observed spatially heterogeneous time series show that these systems are highly variable, at temporal scales of decades that potentially impact some of their marine resources. Based on this standardized data set, we present the effect of global warming at regional level for the three LMEs of Atlantic Africa on SST, wind stress, and primary production. The CCLME and the BCLME are particularly impacted by global warming, especially in their lower latitudes. The GCLME appears "less" impacted according to satellite data when compared to the two other African LMEs, particularly in comparison with the south CCLME where a high SST warming was found. In this study, no significant changes of micronektonic biomass proxy (*i.e.* micronekton acoustic density (S_v in dB)) were observed from 1999 to 2006. As expected, a difference is observed in the vertical micronektonic acoustic density between day and night. However, we observed an unexpected increase in micronekton acoustic density during night-time. Two hypotheses are proposed: (i) the increase is explained by an offshore horizontal diel migration or (ii) a very high contribution of the micronektonic density occurring at the surface (0-10 m), which corresponds to the blind zone of the research vessel. According to an original descriptor "water column filling rate", a significant change in the GCLME is reported. Indeed, there is an increase over the study period of the water column filling rate. Future investigations should focus on this interesting phenomenon. Such an increase should be monitored to inform on a potential major change in the trophic web in this part of the GCLME. These findings can be interpreted as an early warning signal of climate change and require future study.

When we deal with micronektonic trophic levels, using micronekton acoustic scattering layers characteristics is a relevant alternative. Indeed, preliminary results have shown a significant increase (i) of the minimum depth of such scattering layers and (ii) of the mean layer micronektonic density per sampling unit from 1995 to 2015 in the CCLME. Lower daytime S_v values compared to night-time values suggest either less dense patches of micronekton leading to negative day-night differences in the CCLME and GCLME; the kinematic of micronekton behaviour should play a role. Only a few significant and different DVM descriptors suggest a change in the CCLME and the GCLME over the study period. Boosted Regression Tree classification is well suited to show the importance of the large scale environmental variability on micronektonic acoustic density. The inter-annual variability is not significant, showing that the underlying environmental forcing is associated with relatively stable processes. The structural variables, *i.e.*, bathymetry and distance to the coast, consistently explain a

large part of the variability. SST has a minor influence in the north CCLME (consistently cold and windy) and a pronounced effect in the south CCLME where seasonality is high and variable. Especially in Senegal and Guinea, the detrimental effects of the coastal upwelling (mostly offshore drifts due to strong winds) are strongly attenuated by the wider continental shelf which favour retention processes. Considering the oceanographic factors relative influence, and under the assumption of similar warming in the three Atlantic African LMEs, a stronger ecosystem perturbation is expected in BCLME then in the CCLME, particularly when comparing the southern part of the CCLME vs its northern part. In all LMEs, the oceanographic factors' relative influence has a significant role, confirming the important changes expected due to global warming on the ecosystems and thus in the fisheries sector. The next step will be to couple our results with climate projections to forecast major changes in African coastal systems.

Lastly the time series of the DVM amplitude at observed depth in the CCLME indicate not only an increase of the amplitude as a function of time but also a general deepening of the day and night position of the micronekton layer above the slope. Climate features of the time series may reveal a correlation between this behavioural change in amplitude and deepening of the micronekton layer. If a climate-driven change in amplitude and depth is found to be significant, it will have a strong impact on the ocean carbon pump and the climate as the biological production along the slope is generally high. It is expected that a deepening of the micronekton and an increase of the DVM amplitude would enhance the carbon sink and consequently may buffer the carbon dioxide (CO₂) emission in the atmosphere.

Table of content

Table of content.....	5
List of table	6
List of figures.....	6
I.1 Context of Task 12.3.....	10
I.2 Scientific methodology and results.....	10
I.2.1 Survey design in all Large Marine Ecosystems.....	10
I.2.2 Acoustic data processing	12
I.2.3 Environmental data processing	14
I.2.4 Statistical analysis	17
I.2.4.1 Horizontal distribution	18
I.2.4.2 Vertical structure	23
I.2.4.3 Water columns physico-chemical characteristics and influence on layer structure	25
I.2.4.4 The effect of oceanographic factors on micronektonic acoustic density...	37
I.2.4.5 Inter-comparison of Large Marine Ecosystems	37
I.2.4.6 Diel vertical migration of micronekton provides hope: Deepening and amplitude increase may buffer atmospheric carbon dioxide	41
I.3 Perspectives.....	44
I.4 References.....	46
I.5 Appendix.....	48
I.6 Physico-chemical Radial interpolation from CTD probe data	49
I.7 Extra material North GCLME - 2007	64
I.8 Appendix Matecho user manual	71
I.9 Appendix Example of typical echogram processed in this task 12.3	144
I.9.1 Internal waves.....	144
I.9.2 Strong acoustics micronektonic layers	144
I.9.3 DVM Diel Vertical Migration	147
I.10 Appendix Nansen Survey used in the analysis for task 12.3 per LME.....	149
I.10.1 CCLME/ SENEGAL	150
I.10.2 GCLME/ COTE D'IVOIRE.....	150
I.10.3 BCLME/ NAMIBIE.....	151
I.11 Appendix 5: Boosted regression tree cross-validation	152
I.12 Appendix 6: Posters of main WP12.3 results presented at the PREFACE final assembly, 17-20 April 2018, Arrecife, Lanzarote (ES).....	153

List of Tables

Table 1: Number of surveys and distance covered by Nansen surveys studied in this work. The study gather 29 annual surveys and almost 300 000 km of transect surveyed over the three African Atlantic large marine ecosystems (LMEs).	12
Table 2 : extraction criterion of world ocean atlas (WOA).	15
Table 3: Assessment of physico-chemical parameters accuracy based on world ocean atlas (WOA) data.....	16
Table 4: Temporal change of micronekton layers characteristics per large marine ecosystem: CCLME, GCLME and BCLME. No descriptor was found to get significant change in the BCLME while this is the case for CCLME and GCLME. Number of years in the time series: CCLME n = 14; GCLME n = 6 and BCLME n = 8. Green p-values are significant at 0.05 level and orange p-values are significant at 0.1 level.	24
Table 5 : Summary of thermocline correction and final results for the CCLME data base. 28% of the thermocline value have been corrected manually based on expert knowledge. Information available after retreatment represents 79% at least for the minimal depth, 21% corresponds to CTD where the thermocline was not identified.....	26
Table 6 : mean characteristics of thermocline per position vs Cape Blanc (north or south part) and bathymetry (shelf 0-150 m; Slope 150-500 m and plain >500 m).	27
Table 7 : parameters used to model micronektonic acoustic density related to Oceanic factors.....	37
Table 8: Number of elementary sampling unit (ESU of 1 nmi) analysed in the boosted regression tree BRT model, limited by the availability of common acoustics and satellite data, the percentage show the part of acoustics data used in BRT models.	37
Table 9 Results of the DVM amplitude in the CCLME, BCLME, and GCLME between 1995-2015 split into continental shelf, slope, and plain using three different micronekton layer-measures with p-values and the adjusted r^2 (significant increase of DVM amplitude on the slope is marked in red).	44
Table 10. The percentages from each echo-integration cell of the same year and the same LME per class of S_v [in steps of 10 dB around the median] for a year and a given LME. Change of these acoustic population-like over time are tested with a linear regressions per LME (slope and significance). NS : p-value > 0.1; * : 0.1 < p-value < 0.05; ** : 0.05 < p-value < 0.01; *** : p-value < 0.01	45

List of Figures

Figure 1 : Sampling design over time for all surveys considered in this work in the three LMEs (from left to right: CCLME, GCLME, BCLME).	11
Figure 2: Scheme of the Matecho treatment chain step by step. HAC: ICES international standard format for the exchange of raw and edited fisheries acoustics data.	13
Figure 3 : CTD probe localization during Nansen surveys in the Canaries current large marine ecosystem (CCLME). All CTD data have not been released for analysis.	15
Figure 4: Comparison of AVHRR and MODIS sensors for coastal sea surface temperature (SST). Because of possible discrepancies in coastal SST retrieval due to sensor characteristics, calibration, SST algorithms and various atmospheric correction procedures including cloud	

masking, it is important to compare both data sets in the Canary upwelling region. Daytime SST from both AVHRR and MODIS sensors have been compared for the 2003-2012 period (2000-2015 shown). Because limited differences were observed and specially no significant bias, a simple arithmetic average has been performed during this period, minimizing the effect of possible residual differences in the computation of trends over the whole 1982-2015 period in the CCLME. 17

Figure 5: Coastal sea surface temperature (SST) sensibility of spatial averaging. Two ways of spatial averaging were compared for two contrasted areas (area 1, Southern Morocco and area 5, Senegal and Guinea): from the coast to 100 km offshore (the reference chosen in this study) and from the coast to the 200 meter isobath. Slightly lower values of SST are recorded in this case because of the proximity to the coastal upwelling. Nevertheless, the thermal dynamic depicted is identical and do not induce differences in the computation of trends.. 17

Figure 6: Spatial variability of mean S_v in each survey for, from left to right, CCLME, GCLME and BCLME..... 19

Figure 7 : Annual hot and cold spots for, from left to right, CCLME, GCLME and BCLME. 21

Figure 8 : Inter-annual hot and cold spots for, from left to right, CCLME, GCLME and BCLME. 21

Figure 9: Annual acoustic density distribution interpolated by IDW method for, from left to right, CCLME, GCLME and BCLME. 22

Figure 10: Annual acoustic density distribution interpolated by FRK method for, from left to right, CCLME, GCLME and BCLME. 22

Figure 11: Mean vertical profiles calculated for all years together with the standard error represented in dashed lines for, from left to right, CCLME, GCLME and BCLME. 23

Figure 12 : Diel vertical migration profiles calculated for CCLME (in red), GCLME (in blue) and BCLME (in green) for, from left to right, shelf, slope and plain. 23

Figure 13: (A) Filling rate per LME: CCLME Canaries Current (red, n=1'196'698), GCLME Guinea Current (blue, n=664'732) and BCLME Benguela Current (green, n=1'851'228). (B) Filling rate contribution of the first layer per LME: CCLME Canaries Current (red, n=992'737), GCLME Guinea Current (blue, n=166'183) and BCLME Benguela Current (green, n=426'807). (C) Layer number by ESU per LME: CCLME Canaries Current (red, n=869'307), GCLME Guinea Current (blue, n=156'642) and BCLME Benguela Current (green, n=402'951). 24

Figure 14 : Position of hypoxia in the water column ($< 1 \text{ ml l}^{-1}$ of dissolved oxygen in the water) observed on the CTD probe data base in Senegal and over the CCLME in 1998, 1999, 2000 and 2001. On the right, box plot of the percentage of water column above our hypoxia threshold per year in Senegal for the same time series. 25

Figure 15 : Examples of thermocline characterization without correction (red lines) and manual correction (green lines) for CTD 1130 and 1136 collected in 1998. 26

Figure 16 : scatterplot of thermocline altitude (m) according to the bottom depth (m) in the north and south of CCLME (split according to Cap Blanc position i.e. $20^{\circ}46'13'' \text{ N}$). The first bisector ($X=Y$) is drawn in red. 27

Figure 17 : scatterplot of thermocline minimal depth (m) according to the bottom depth (m) in the north and south of CCLME (split according to Cap Blanc position i.e. $20^{\circ}46'13'' \text{ N}$). The first bisector ($X=Y$) is drawn in red. 28

Figure 18 : Boxplot of micronekton acoustic density (S_v) distribution in daytime (left) and nighttime (right) in southern CCLME per year and layers' position related to the thermocline (red for "above", green for "below" and blue for "in"). Boxplot width is proportional to the number of layer (N) detected by year. Outliers are not display. North and south of CCLME are split according to Cap Blanc position i.e. $20^{\circ}46'13''$ N. 29

Figure 19 : Boxplot of micronekton acoustic density (S_v) distribution in daytime (left) and nighttime (right) in northern CCLME declined by year and layers' position to thermocline (red for above, green for below and blue for in). Boxplot width is proportional to the number of layer detected by year (N). Outliers are not drawn. North and south of CCLME split vs Cap Blanc position i.e. $20^{\circ}46'13''$ N. 30

Figure 20 : Physico-chemical parameters profiles identified using k-means clustering in the CCLME. Three group appear for the temperature and two for the salinity as well as oxygen. Group 1 in black corresponds to the north (Figure 21) of CCLME, group 2 in red, group 3 in green are associated spatially to the south part. 31

Figure 21: Localization of K-means clusters. Group 1 in black, group 2 in red, group 3 in green along the CCLME for each parameters (temperature, salinity and oxygen), report to Figure 20. 32

Figure 22 : CCLME south mean profile of temperature (red), oxygen (blue) and salinity (orange). In background, layer presence probability is drawn by cluster at each depth with night (dark grey) and day (light grey) contributions. Each graphic correspond a cluster discriminated by the K-means (Fig. 20). 33

Figure 23 : CCLME north mean profile of temperature (red), oxygen (blue) and salinity (orange) see Figure 20 for their position. In background, layer presence probability is drawn by cluster at each depth with night (dark grey) and day (light grey) contributions. 34

Figure 24: CCLME (up) north CCLME and south (down) mean profile of temperature (red), oxygen (blue) and salinity (orange). In background, layer presence probability is drawn by cluster at each depth with night (dark grey) and day (light grey) contributions, for S_v below - 65dB. 35

Figure 25: CCLME (up) north CCLME and south (down) mean profile of temperature (red), oxygen (blue) and salinity (orange). In background, layer presence probability is drawn by cluster at each depth with night (dark grey) and day (light grey) contributions, for S_v above - 65dB. 36

Figure 26 : Inter large marine ecosystem comparison of S_v anomalies based on inter-annual S_v mean of each LME subtracted at each year from 1994 to 2015. 39

Figure 27 : correlation circle with (a) all variables, (b) only selected variables. Coulour (\cos^2) gives the contribution of two first axis. Profondeur = depth, moyenne = mean, prof max = depth max. 40

Figure 28: Cloud of dots with selected variables. Illustrative variable (points colour) is the large marine ecosystems. 41

Figure 29 : Mean micronekton layer widths in the CCLME at (1) day and (2) night split into bathymetric areas (a) shelf, (b) slope, and (c) plain between 1995-2015. GCLME and BCLME get too short time series to be efficiently analysed. 43

Figure 30 : Time series of the DVM amplitude in the CCLME on the slope between 1995-2015 using three different micronekton layer-measures (a) maximum, (b) mean, (c) minimum. .. 43

Figure 31 : Time series of the DVM amplitude at observed depth in the CCLME on the slope between 1995-2015 using three different micronekton layer-measures (a) maximum, (b) mean, (c) minimum; the top of the bar = mean night position; the bottom of the bar = mean day position.	44
Figure 32 : Top : change in acoustic population-like per class of 10 dB in each large marine ecosystems (CCLME, GCLME and BCLME) express in percentage cells of a same class. Down: change of micronekton barycenter in the north and south of Cap Blanc in Canaries Current large marine ecosystem (CCLME). No significant shift appear even if a small trend toward the north can be suspected according to 2015 vs 1995 latitudinal position.	46
Figure 33 : Internal wave at 100-200 m. Namibia June 2009.	144
Figure 34 : Strong signal of internal waves in surface. Namibia August 1999.....	144
Figure 35 : Convergence of layers under internal waves effect. Namibia June 1997.....	144
Figure 36 : Internal waves in shallow water Namibia June 1997.....	144
Figure 37 : Strong Layer (18 kHz). Namibia August 1999.....	145
Figure 38 : Strong layer at 50-150 m sharply define; Namibia June 1997.....	145
Figure 39 : Big fish school (in red). Sénégal May 2002.....	145
Figure 40 : Strong layers 200 et 300 m. Sénégal Septembre 2000.	145
Figure 41 : Surface layer and layer at 200 m with empty space. Sénégal September 2000..	145
Figure 42 : Strong layer at 250 m. Sénégal May 2001.	145
Figure 43 : Layer in surface and then at 100 m. Sénégal September 2000	146
Figure 44 : Water column full 20-300m. Sénégal 2002.....	146
Figure 45 : layer strongly constraint by the environment and with internal wave. Namibia June 1997.	146
Figure 46 : String layer in the bottom (300 m) Namibia June 1998.....	146
Figure 47 : Strong layer blocked before the bottom (100 m). Namibia September 1999.....	146
Figure 48 : Migration of a layer not linked to a diel vertical behaviour (around 12:00). Sénégal 2001.....	146
Figure 49 : DVM dusk, Sénégal 2000.....	147
Figure 50 : DVM sunset. Sénégal 2000.....	147
Figure 51 : DVM night with internal wave. Sénégal summer 2012	147
Figure 52 : DVM in the morning. Namibia June 1997	147
Figure 53 : Echo integrated DVM sunset which reach the surface. Layer not migrant at 200-300 m. Sénégal summer 2012.....	147
Figure 54 : Echo integrated DVM dusk and dawn around the shelf. Sénégal summer 2012	147
Figure 55 : Echo integrated DVM dusk and dawn. Sénégal summer 2000	147
Figure 56 : Echo integrated DVM dusk and dawn. Sénégal summer 2000	148
Figure 57 : DVM sunset. Sénégal Summer 2012	148